


## ORIGINAL ARTICLE OPEN ACCESS

# Development of AI Based Fibrosis Detection Algorithm by SHG/TPEF Microscopy for Fully Quantified Liver Fibrosis Assessment in MASH

Kutbuddin Akbary<sup>1</sup>  | Mazen Nouredin<sup>2</sup> | Ren Yayun<sup>1</sup> | Dean Tai<sup>1</sup> | Pol Boudes<sup>3</sup><sup>1</sup>HistoIndex Pte Ltd, Singapore, Singapore | <sup>2</sup>Houston Methodist Hospital, Houston, Texas, USA | <sup>3</sup>Rectify Pharmaceuticals, Cambridge, Massachusetts, USA**Correspondence:** Pol Boudes ([pboudes@rectifypharma.com](mailto:pboudes@rectifypharma.com))**Received:** 22 April 2025 | **Revised:** 23 June 2025 | **Accepted:** 24 July 2025**Handling Editor:** Salvatore Petta**Funding:** The authors received no specific funding for this work.**Keywords:** artificial intelligence | fibrosis | Machine Learning | MASH | MASLD

## ABSTRACT

**Background and Aims:** Metabolic dysfunction-associated steatotic liver disease (MASLD) is a major global cause of chronic liver disease, with the potential to progress from steatosis to metabolic dysfunction-associated steatohepatitis (MASH) and cirrhosis. Fibrosis is a key determinant of liver-related morbidity and mortality, highlighting the need for precise, reproducible assessment methods. This study aimed to develop and validate an Artificial Intelligence (AI)-based fibrosis detection algorithm using Second Harmonic Generation/Two Photon Excitation Fluorescence (SHG/TPEF) microscopy.

**Methods:** The algorithm integrates SHG/TPEF microscopy, which uses ultra-fast lasers to capture intrinsic optical signals from unstained liver biopsies, with Machine Learning (ML)-based image analysis. The resulting qFibrosis model quantifies collagen morphology to generate a continuous fibrosis index.

**Results:** A standardised workflow was established, encompassing sample acquisition, SHG/TPEF imaging, region-specific analysis and collagen feature quantification. Each step of the AI-based ML of qFibrosis algorithm used to assess and quantify liver fibrosis is described in detail in this study.

**Conclusions:** This AI-driven approach enables accurate, continuous quantification of liver fibrosis, overcoming the variability of traditional histopathology. The qFibrosis model has potential as a standardised tool for therapeutic evaluation and disease monitoring in MASLD/MASH, representing a significant advancement in liver fibrosis assessment.

## 1 | Background and Aims

Metabolic dysfunction associated steatotic liver disease (MASLD) is a significant global contributor to chronic liver disease, exhibiting a prevalence ranging from 20% to 30% across

diverse regions [1, 2]. This condition spans from liver steatosis to metabolic dysfunction-associated steatohepatitis (MASH). The latter is characterised histologically by hepatocellular injury, inflammation and fibrosis. Fibrosis assessments in liver biopsies are commonly used in determining liver-related morbidity and

**Abbreviations:** AI, artificial intelligence; AUROC, area under the receiver operating characteristic; CART, classification and regression tree; CPA, collagen proportionate area; MASH, metabolic dysfunction-associated steatohepatitis; MASLD, metabolic dysfunction-associated steatotic liver disease; ML, Machine Learning; NASH-CRN, nonalcoholic steatohepatitis clinical research network; SHG/TPEF, Second Harmonic Generation/Two-Photon Excitation Fluorescence.

This is an open access article under the terms of the [Creative Commons Attribution-NonCommercial-NoDerivs](https://creativecommons.org/licenses/by-nc-nd/4.0/) License, which permits use and distribution in any medium, provided the original work is properly cited, the use is non-commercial and no modifications or adaptations are made.

© 2025 The Author(s). *Liver International* published by John Wiley & Sons Ltd.

## Summary

- This study introduces a new AI-based method to measure liver scarring (fibrosis) more accurately in patients with fatty liver disease.
- Using advanced laser imaging and ML, the system analyses tissue samples without the need for staining and provides a detailed, consistent fibrosis score.
- This approach could help doctors better track disease progression and evaluate treatment responses.

mortality [3]. MASH, if left untreated, can progress to liver cirrhosis, which may require liver transplantation [4–8]. In order to develop new therapeutic agents for the treatment of MASH, one of the key clinical efficacy endpoints requested by regulators in MASH drug trials is the reduction of fibrosis on liver biopsies. This is defined by at least a decrease of 1 stage on the NASH-CRN classification [9]. The semi-quantitative NASH-CRN staging is based on specific tissue staining and classifies fibrosis from stage 0 to stage 4 (cirrhosis) [3, 10–12]. The NASH-CRN system, however, depends on slides preparation and staining quality, has limited precision, and is poorly reproducible [13, 14]. This underscores the need for an improved, standardised, continuous quantitative measurement of liver fibrosis to evaluate candidate drugs therapeutic responses.

Recent breakthroughs in ultra-fast lasers have enabled the imaging of intrinsic optical signals through Second Harmonic Generation (SHG) auto-fluorescence and Two-Photon Excitation Fluorescence (TPEF). Moreover, these advanced imaging technologies are complemented by Artificial Intelligence (AI) based tools such as Machine Learning (ML), for enhanced analysis and interpretation of the SHG/TPEF images. Furthermore, these technologies can be applied to unstained biopsy slides, as such eliminating one important component of variability. Previous studies have introduced the SHG-based Quantification of Fibrosis-related Parameters (Q-FP) model in unstained liver biopsies, which have provided a better assessment of collagen architectural changes and produced a continuous, quantitative fibrosis scale [15]. Subsequent studies combining SHG and TPEF microscopy to quantify collagen deposition provided further improvements to create the quantitative qFibrosis system [16, 17].

Ideally, two sequential tissue sections from the tissue block, one stained and one unstained, can be used to enable direct comparison between pathologist-based fibrosis assessments and qFibrosis respectively, enabling both MASH diagnosis and accurate collagen quantification using qFibrosis.

Recent data [18] shows that regression and progression in MASH are subtle and specific to certain lobular and portal zones of the liver. SHG/TPEF imaging-based AI-ML analysis provides qFibrosis, which demonstrates higher sensitivity than human interpretation in capturing these subtle zonal changes. ML, a subset of AI, allows computer systems to autonomously learn and enhance from experience, enabling tasks such as image segmentation, classification, and quantitative analysis by recognising patterns and features within the generated images. Here we describe the SHG/TPEF scanning and imaging of unstained liver biopsy slides, and

provide comprehensive details on the acquisition, analysis, processing and validation of qFibrosis measurements.

## 2 | Methods

The process workflow of qFibrosis, as depicted in the flow-chart (Figure 1), will be described in a step-by-step manner subsequently.

Sample acquisition is done when formalin fixed unstained liver tissue is paraffin embedded, then sectioning of this tissue (taken separately from the section of liver biopsy tissue used for subsequent staining) is done of approximately 4–5  $\mu\text{m}$  thickness and mounted on glass slides, as per standard Formalin Fixed Paraffin Embedded procedure. These slides are first inspected by a trained operator to ensure that the dimensions and quality of tissue are optimal for imaging and subsequent analyses. There should only be one patient's tissue sample per slide. The slides are then deparaffinised as per standard protocols before being scanned. Image acquisition is performed with a 20 $\times$  objective lens on these unstained and deparaffinised biopsy slides.

The process of 'Laser Staining' utilises the Genesis200 (HistoIndex Pte. Ltd., Singapore), which is a laser-based multiphoton fluorescence imaging microscope, where the SHG signal detector is used to visualise collagen and the TPEF signal detector is used to visualise other histological structures, such as hepatocytes, inflammatory cells and biliary epithelium (Figure 2). The samples are laser excited at 780 nm, SHG signals are recorded at 390 nm, and TPEF signals are recorded at 550 nm. Images are acquired with 512  $\times$  512-pixel resolution in dimensions of 200  $\mu\text{m}$   $\times$  200  $\mu\text{m}$  tiles, resulting in 1 pixel being equivalent to 0.3906  $\mu\text{m}$ . Multiple adjacent image tiles are captured to encompass the whole tissue area in each biopsy sample. In the final images, collagen regions are indicated in green colour and hepatocyte regions are indicated in red colour (Figure 3). Images obtained from the TPEF detector (Figure 3B) and the SHG detector (Figure 3C) are further combined to produce the final image of the biopsy as seen in Figure 3D.

'Machine Learning Staining' is a combination of SHG and TPEF microscopy and has further processes as a part of each of these image microscopies (Figure 4), which shall be described stepwise below. SHG imaging comprises of Steps A, B and C, whereas TPEF imaging comprises of Steps D, E and F.

## 3 | Results

Collagen detection (Step A) is first achieved with the SHG imaging channel using Otsu's automatic threshold method [19]. SHG imaging allows automatic identification of collagen within the tissue to be analysed (Figure 4A). The Collagen Proportionate Area (CPA) is quantified based on the SHG signal detected. Collagen segmentation (Step B) is where the tissue image having a collagen area smaller than 15  $\mu\text{m}^2$  is labelled as noise and is eliminated from total collagen quantification (Figure 4B).

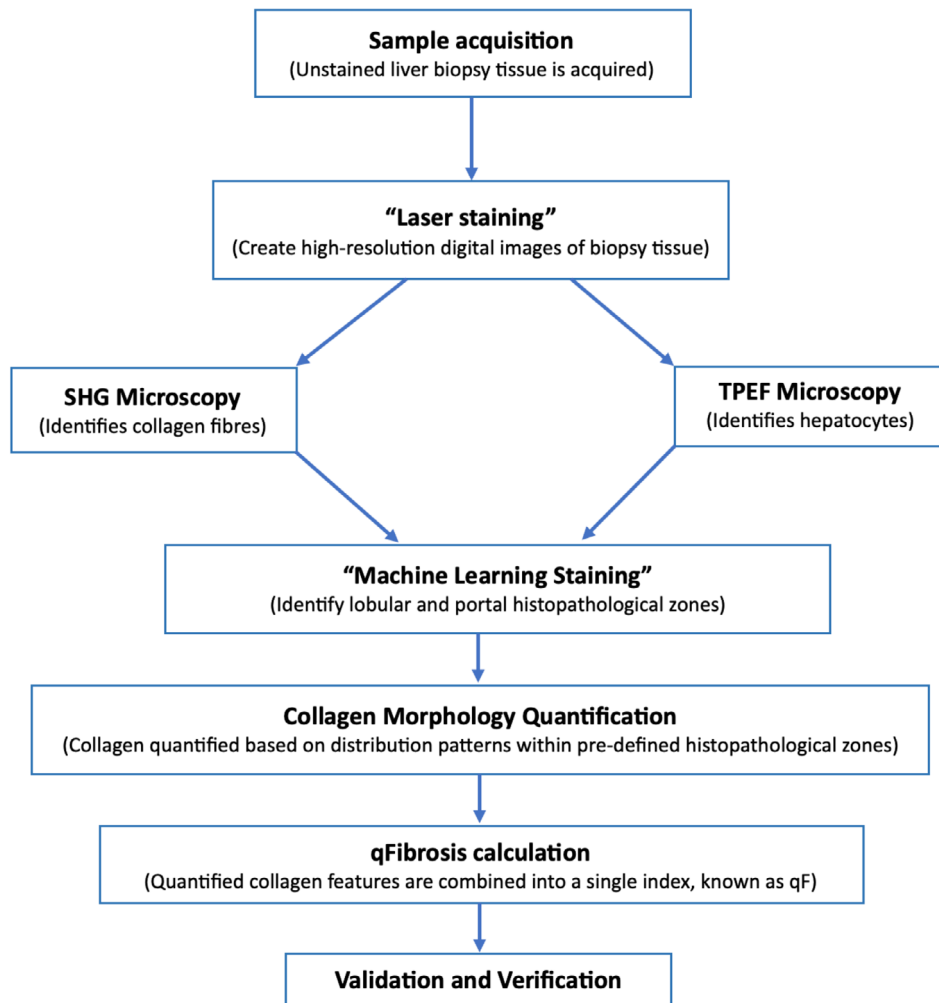


**FIGURE 1** | Flowchart describing the process workflow.

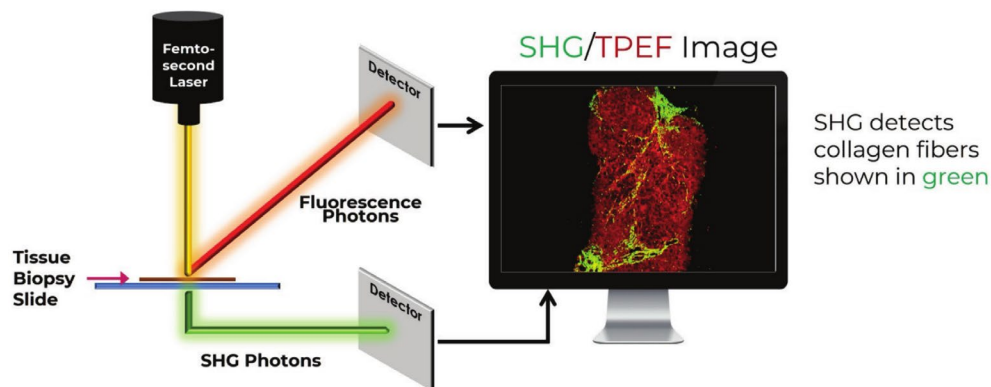


**FIGURE 2** | Simplified Genesis200 imaging platform.

Connected component analysis to identify collagen linked to vessels (Step C) involves employing morphological closing and opening techniques to eliminate small collagen areas while retaining the shape and size of larger collagen regions [20]. Morphological closing helps to fill in small gaps and smooth out irregularities in collagen regions, while morphological opening removes small isolated regions without significantly altering the overall shape and size of larger collagen structures. This process ensures that only relevant collagen features are retained for

further analysis. Determination of collagen surrounding vessels relies on identifying large collagen components connected to the vessels (Figure 4C).

The process of determination of tissue to be analysed (Step D) is performed in TPEF imaging channel (Figure 4D). The Otsu's automatic threshold method is applied to locate all tissue locations. Tissue components or regions that are considered artefacts or not necessary for analysis of fibrosis are excluded. Regions

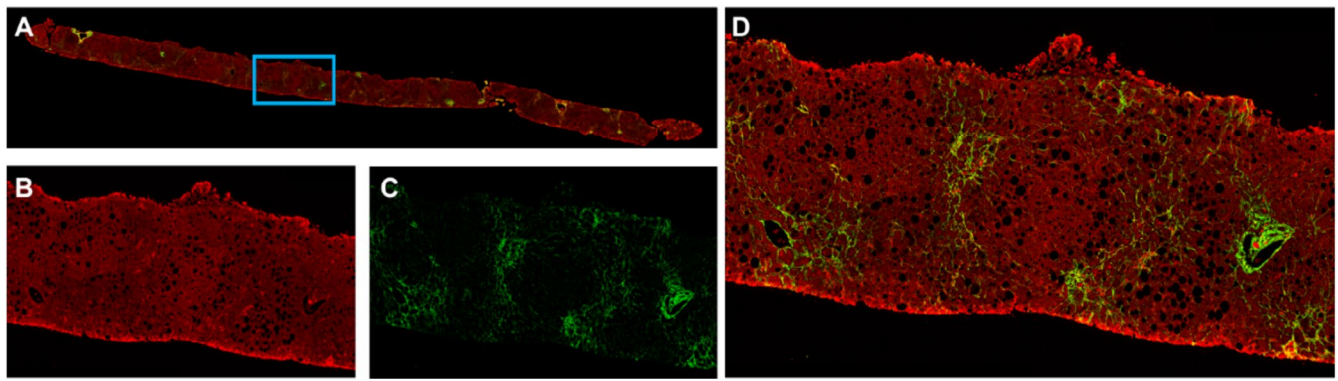


**FIGURE 3** | Examples of Laser Staining. (A) SHG/TPEF image for an unstained liver biopsy. The blue box is further expanded for detailed viewing in (B–D). (B) Shows TPEF microscopy-based imaging (delineation of hepatocytes, indicated in red). (C) Shows SHG microscopy-based identification of fibrosis (indicated in green). (D) Combined image.

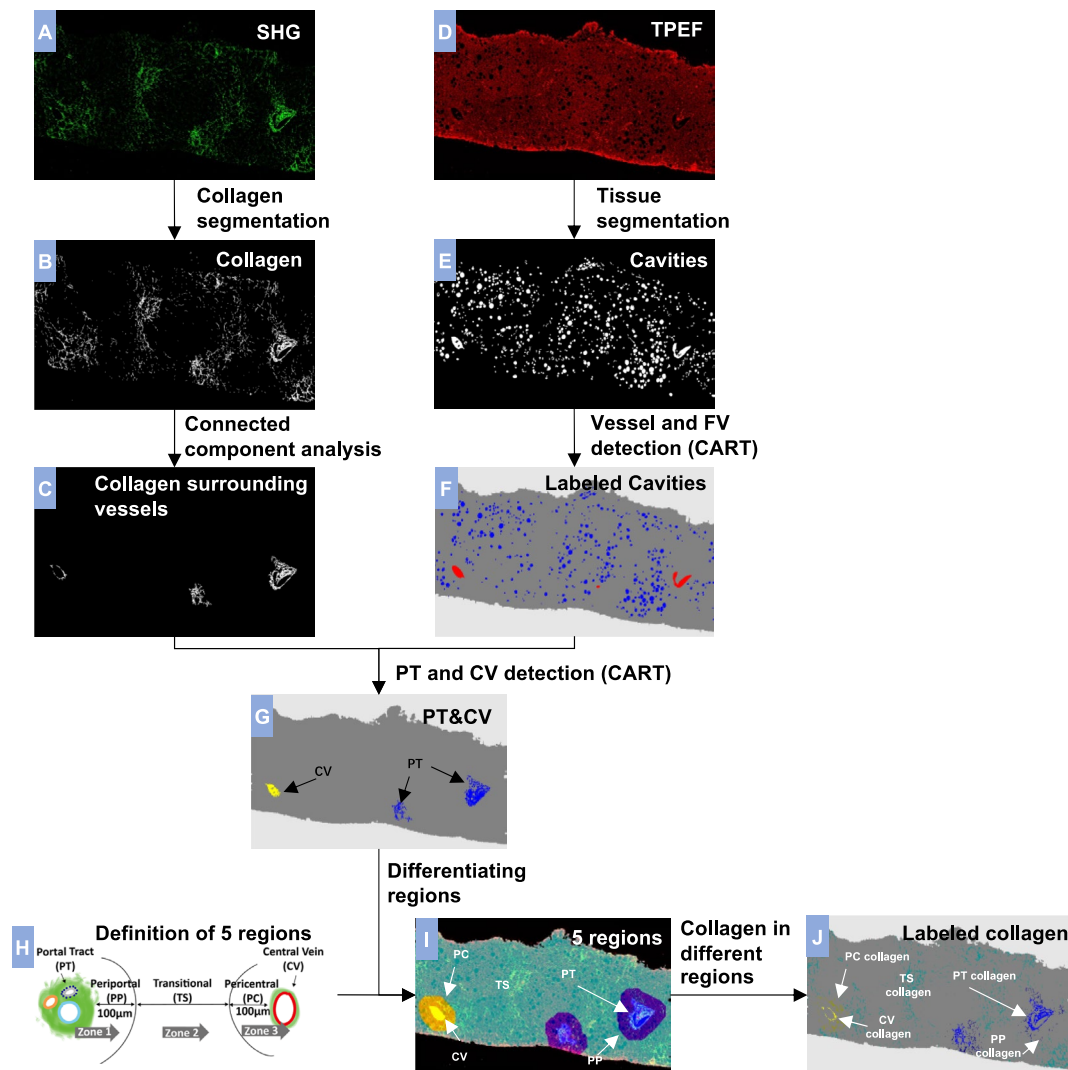


**FIGURE 4** | Sequential execution of steps (A–J) included in 'Machine Learning staining'. The details of each step are described in the subsequent passages.

greater than  $0.1 \text{ mm}^2$  are identified as the tissue region. Noise removal involves recognising and eliminating TPEF signals outside the tissue region.

For Tissue Segmentation (Step E), within biopsy tissue, various anatomical structures such as vessels, bile ducts, steatosis, hepatic sinusoids and unnatural cracks are detected from the



TPEF channel. They are labelled as cavities, and no signal will be measured in these structures (Figure 4E). This process helps in identifying all the cavities in the scanned image.

Pathologist annotations on corresponding stained biopsy sections were used to identify key regional landmarks such as portal tracts, central veins and steatosis areas. These annotations served as training data for the algorithm's vessel/fat vacuole detection and PT/CV classification tasks, focusing on broader architectural features rather than detailed labeling of individual structures like blood vessels or bile ducts. Vessel and Fat Vacuole detection (Step F) is where a decision tree constructed using the Classification And Regression Tree (CART) method [21] distinguishes cavities caused by vessels, bile ducts and steatosis based on specific features, such as the density of cavities, width and length of cavities, cavity opacity and the area of surrounding collagen of cavities (Figure 4F). This process helps in classifying all cavities that have been detected in the previous step. The selection of the regions of interest is depicted by Steps G and H. In this step, information and images from collagen evaluation (Step C) and tissue segmentation and cavities identification (Step F) are combined in Step G (Figure 4G).

PT and CV detection (Step G) is where a decision tree method called Classification and Regression Tree (CART) is employed to differentiate between Portal Tract (PT) and Central Vein (CV) regions within the liver tissue. Various features, including number and size of tissue cavities, extent of collagen deposition and distances between tissue cavities and surrounding collagen, are used as criteria to delineate these regions of interest.

For Differentiating Regions (Step H), after identifying PT and CV regions, Peri-Portal (PP) and Peri-Central (PC) regions can be determined. The PP region is defined as being within  $100\mu\text{m}$  around the portal tract, while PC is defined as being within  $100\mu\text{m}$  around the central vein. The transitional region (TS) is the remaining region excluding PT, CV, PP and PC from the overall tissue. These definitions have been defined based on inputs from expert liver pathologists (Figure 4H).

The output image from this process of differentiating regions based on pre-defined anatomical regions is depicted in Figure 4I. After identifying PT, PP, TS, PC and CV regions,

collagen detected within these pre-defined regions is labelled as PT collagen, PP collagen, TS collagen, PC collagen and CV collagen (Figure 4J). Once collagen has been identified and divided into pre-defined anatomical regions, the process of quantifying collagen is initiated and the following steps are followed to derive a continuous parameter, the qFibrosis value, that fully quantifies tissue collagen content.

All collagen fibres identified (Figure 5A) can be distinguished into aggregated and distributed (non-aggregated) collagen fibres. The thinning algorithm determines the skeleton of the collagen image. In image processing, the 'thinning algorithm' is a computational method used to reduce the thickness of objects in an image while preserving their shape and connectivity [22]. In SHG/TPEF imaging analysis, the thinning algorithm specifically operates on the collagen image, extracting a simplified representation known as the 'skeleton'. This skeleton captures the essential structure of collagen fibres, facilitating further analysis. Aggregated collagen fibres include at least 2 branches according to the skeleton. Intersections between branches are recognised and counted in aggregated collagen fibres (Figure 5B). Consequently, collagen fibres that have no intersections among themselves are defined as distributed (non-aggregated) collagen fibres. Connected component analysis is utilised to calculate morphological features, such as area, perimeter, length and width for aggregated and distributed fibres, respectively (Figure 5C). Connected component analysis is employed to identify and analyse the morphological features of collagen fibres within liver biopsy images. This process involves grouping adjacent pixels or regions that share similar properties, such as intensity or colour, into connected components. By segmenting collagen fibres based on their connectivity, this analysis enables the calculation of key morphological parameters of collagen, such as area, perimeter, length and width, which are essential for quantifying fibrosis in the biopsy. Identification of long fibres (length  $> 20\mu\text{m}$ ) and thick fibres (width/length ratio  $> 0.25$ ) is done based on definitions provided by liver pathologists. Calculation of the number of long fibres, short fibres, thick fibres and thin fibres for aggregated and distributed fibres, respectively, is then performed. Overall collagen parameter values in each region (PT/PP/TS/PC/CV) are calculated by adding up collagen in aggregated and distributed fibres. Overall parameter values for the entire tissue are then calculated by adding up PT, PP, TS, PC and CV region collagen. Collagen morphological parameters are

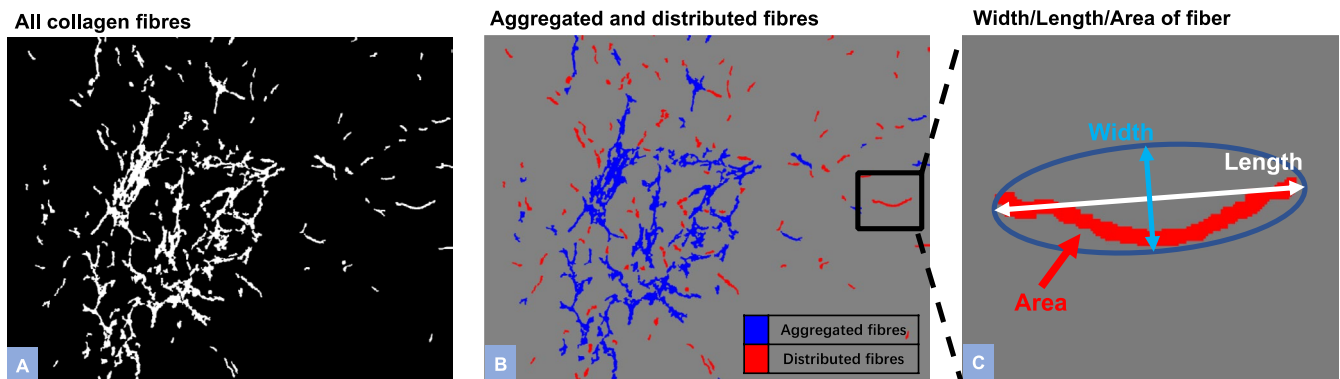


**FIGURE 5** | (A) Illustrates all identified collagen fibres. (B) Intersections among branches are identified and quantified within the aggregated collagen fibres. (C) Connected component analysis is used to compute various collagen morphological features such as area, perimeter, length and width for aggregated and distributed fibres, respectively.

quantified by the area of the entire tissue and normalised by dividing it by its maximum value.

For the qFibrosis Calculation process, initial steps involve quantifying collagen parameters for a specific set of training samples. These parameters, along with their corresponding NASH-CRN fibrosis stages, undergo a sequential feature selection method [23] to streamline the dataset by identifying the most informative collagen morphological parameters. Subsequently, the selected collagen parameters are utilised to train a qFibrosis model, employing a linear regression approach to generate qFibrosis continuous values. These continuous values serve as indicators of liver fibrosis severity in patients with MASLD.

While qF continuous values represent the primary output of comprehensive collagen quantification in liver biopsies and are also one of the major advantages of this form of fibrosis evaluation, they can also be organised into semi-quantitative stages, termed qFibrosis stages (qF0, qF1, qF2, qF3 and qF4), using predefined cut-off values to aid clinical interpretation. These qFibrosis stages correspond to the NASH-CRN fibrosis stages, ensuring comparability with established clinical staging frameworks.

Verification of qFibrosis Algorithm is performed to ensure its accuracy and reliability wherein a rigorous verification process is undertaken. This involves an independent coder developing

**TABLE 1** | Verification data demonstrating the concordance of biopsies as per qFibrosis algorithm stages with the stages derived from the new algorithm (independent coder algorithm).

qFibrosis stage	qFibrosis algorithm biopsies	Independent coder algorithm staged biopsies
qF0	11	13
qF1	2	0
qF2	11	11
qF3	10	10
qF4	14	14

Note: The agreement between the qF stage and the independent coder algorithm stage is 95.8%, with 46 out of 48 biopsy stage readouts.

their own algorithm based on descriptions provided in previous sections. A set of liver biopsy images, comprising MASH liver biopsy samples from a clinical study ( $n=48$ ) [24], is then provided to both the qFibrosis algorithm and the new algorithm developed by the independent coder. Successful verification is achieved when there is over 95% agreement in the qFibrosis stage results generated by both algorithms. An actual example of verification data is included in Tables 1 and 2.

Additionally, software verification is conducted to ensure that the implemented software functions according to its design documents, with verification performed after each implementation or integration phase. Verification of qFibrosis measurement Graphic User Interface involves confirming that its functionality aligns with the Operator's Manual, while verification of qFibrosis analysis functionality entails validating that the algorithm generates a final qFibrosis value as described in previous sections.

The qFibrosis algorithm also incorporates version control and standardised validation protocols to address the issue of algorithm stability. All modifications undergo rigorous testing using a fixed holdout dataset of biopsy images with pathological reading, ensuring changes do not compromise the reproducibility of prior findings. For studies using earlier versions, documentation of algorithm iterations (e.g., version number, validation metrics and training data updates) is done, allowing transparent comparison across different versions. While incremental improvements are expected, core structural features (e.g., portal tract/central vein localization, collagen quantification) which are critical for fibrosis staging are preserved to maintain consistency with historical analyses. This approach balances methodological rigour with adaptability.

Subsequently, validation of the qFibrosis algorithm is essential to confirm its ability to meet the requirements of its intended use. Furthermore, the qFibrosis model undergoes validation across cohorts participating in various MASH drug trials utilising the NASH-CRN system for liver biopsy assessments. Performance evaluation includes assessing agreement between qFibrosis and NASH-CRN fibrosis stages through metrics such as area under the receiver operating characteristic (AUROC) analysis, Spearman's correlation analysis and Cohen's kappa statistic. This validation process ensures the creation of a reliable and reproducible index for fibrosis assessment. Upon confirmation of satisfactory performance in correlation with pathologist-based

**TABLE 2** | Illustrates the variance in qFibrosis continuous values between the qFibrosis algorithm and the Independent coder algorithm, with SD denoting Standard Deviation.

qFibrosis stage	Absolute difference	Relative difference
	Mean (SD)	Mean (SD)
qF0 ( $n = 11$ )	0.03 (0.03)	5.71% (6.34%)
qF1 ( $n = 2$ )	0.04 (0.02)	4.40% (2.88%)
qF2 ( $n = 11$ )	0.03 (0.02)	2.33% (1.66%)
qF3 ( $n = 10$ )	0.02 (0.02)	1.28% (0.99%)
qF4 ( $n = 14$ )	0.04 (0.03)	1.19% (0.69%)
Overall	0.03 (0.03)	2.64% (3.72%)

Note: Analysis is used to compute various collagen morphological features such as area, perimeter, length and width for aggregated and distributed fibres, respectively.

readouts, the algorithm is finalised for application in different MASH drug trials.

Clinical validation of the newly developed qFibrosis value will entail assessing its performance against established clinical features of MASH. Specifically, its correlation with and predictive ability for clinical outcomes, such as liver decompensation or survival, will serve as the reference standard for its validation, enabling its use as a surrogate fibrosis assessment standard in MASH clinical trials. Additionally, longitudinal studies tracking disease progression in MASH patients will validate the effectiveness of qFibrosis values in monitoring fibrosis evolution over time. By demonstrating strong concordance with these clinical features, qFibrosis values can establish themselves as a reliable tool for assessing and managing liver fibrosis in MASH patients. Clinical validation of qFibrosis with extensive MASH natural history cohorts is presently in progress. Future studies could also explore associations between qFibrosis-based assessments and subdivisions within fibrosis classifications, such as F1a, F1b and F1c, potentially utilising collagen morphometry to further align with pre-existing classification systems such as NASH-CRN.

## 4 | Conclusions

In conclusion, we outline a comprehensive approach to liver fibrosis assessment in MASLD/MASH through the integration of advanced imaging techniques and AI. The combination of SHG/TPEF imaging, facilitated by ultra-fast lasers, offers a nuanced understanding of collagen architectural changes in MASLD/MASH. The development and application of the qFibrosis model, incorporating Laser-staining and ML staining along with quantification algorithms, provide a continuous and quantitative scale for fibrosis evaluation.

The sequential development of qFibrosis index, described in a comprehensive flowchart and indicative images, not only provides a blueprint for future AI digital pathology platforms but also contributes to the ongoing efforts in standardising and refining histopathological assessment. The outlined workflow and methodologies provide a clear path for developing an AI-based algorithm for assessing liver fibrosis, offering a foundation for further research and the creation of more effective parameters to better assess the outcomes in therapeutic strategies for MASLD/MASH.

---

### Author Contributions

Study design: All authors. Study conduct: All authors. Preparation of the manuscript: Kutbuddin Akbary, Pol Boudes, Yayun Ren. Critical review of the manuscript: All authors. All authors approved the final version of the manuscript.

### Ethics Statement

The authors have nothing to report.

### Consent

The authors have nothing to report.

### Conflicts of Interest

M.N. reports consulting agreements and research support from several pharmaceutical companies but none represent a potential conflict for this paper. K.A., R.Y. and D.T. are employees of HistoIndex Pte Ltd., Singapore. P.B. is an employee of Rectify Pharmaceuticals Inc.

### Data Availability Statement

The data that support the findings of this study are available from the corresponding author upon reasonable request.

### References

1. Z. M. Younossi, A. B. Koenig, D. Abdelatif, Y. Fazel, L. Henry, and M. Wymer, "Global Epidemiology of Nonalcoholic Fatty Liver Disease: Meta-Analytic Assessment of Prevalence, Incidence, and Outcomes," *Hepatology* 64 (2016): 73–84.
2. Z. Younossi, Q. M. Anstee, M. Marietti, et al., "Global Burden of NAFLD and NASH: Trends, Predictions, Risk Factors and Prevention," *Nature Reviews. Gastroenterology & Hepatology* 15 (2018): 11–20.
3. P. S. Dulai, S. Singh, J. Patel, et al., "Increased Risk of Mortality by Fibrosis Stage in Nonalcoholic Fatty Liver Disease: Systematic Review and Meta-Analysis," *Hepatology* 65 (2017): 1557–1565.
4. M. R. Charlton, J. M. Burns, R. A. Pedersen, K. D. Watt, J. K. Heimbach, and R. A. Dierkhising, "Frequency and Outcomes of Liver Transplantation for Nonalcoholic Steatohepatitis in the United States," *Gastroenterology* 141 (2011): 1249–1253.
5. R. J. Wong, R. Cheung, and A. Ahmed, "Nonalcoholic Steatohepatitis Is the Most Rapidly Growing Indication for Liver Transplantation in Patients With Hepatocellular Carcinoma in the U.S," *Hepatology* 59 (2014): 2188–2195.
6. N. Kemmer, G. W. Neff, E. Franco, et al., "Nonalcoholic Fatty Liver Disease Epidemic and Its Implications for Liver Transplantation," *Transplantation* 96 (2013): 860–862.
7. R. J. Wong, M. Aguilar, R. Cheung, et al., "Nonalcoholic Steatohepatitis Is the Second Leading Etiology of Liver Disease Among Adults Awaiting Liver Transplantation in the United States," *Gastroenterology* 148 (2015): 547–555.
8. Z. M. Younossi, R. Loomba, Q. M. Anstee, et al., "Diagnostic Modalities for Nonalcoholic Fatty Liver Disease, Nonalcoholic Steatohepatitis, and Associated Fibrosis," *Hepatology* 68 (2018): 349–360.
9. US Department of Health and Human Services Food and Drug Administration Center for Drug Evaluation and Research, "Noncirrhotic Nonalcoholic Steatohepatitis With Liver Fibrosis: Developing Drugs for Treatment," Guidance for Industry [Draft Guidance], 2018, <https://www.fda.gov/regulatory-information/search-fda-guidance-documents/noncirrhotic-non-alcoholic-steatohepatitis-liver-fibrosis-developing-drugs-treatment>.
10. H. Hagström, P. Nasr, M. Ekstedt, et al., "Fibrosis Stage but Not NASH Predicts Mortality and Time to Development of Severe Liver Disease in Biopsy-Proven NAFLD," *Journal of Hepatology* 67 (2017): 1265–1273.
11. P. Angulo, D. E. Kleiner, S. Dam-Larsen, et al., "Liver Fibrosis, but no Other Histologic Features, Is Associated With Long-Term Outcomes of Patients With Nonalcoholic Fatty Liver Disease," *Gastroenterology* 149 (2015): 389–397.e10.
12. M. Ekstedt, H. Hagström, P. Nasr, et al., "Fibrosis Stage Is the Strongest Predictor for Disease-Specific Mortality in NAFLD After up to 33 Years of Follow-Up," *Hepatology* 61 (2015): 1547–1554.
13. S. Astbury, J. I. Grove, D. A. Dorward, I. N. Guha, J. A. Fallowfield, and T. J. Kendall, "Reliable Computational Quantification of Liver

Fibrosis Is Compromised by Inherent Staining Variation,” *Journal of Pathology. Clinical Research* 7, no. 5 (2021): 471–481.

14. B. A. Davison, S. A. Harrison, G. Cotter, et al., “Suboptimal Reliability of Liver Biopsy Evaluation has Implications for Randomized Clinical Trials,” *Journal of Hepatology* 73, no. 6 (2020): 1322–1332.

15. Y. Wang, R. Vincent, J. Yang, et al., “Dual-Photon Microscopy-Based Quantitation of Fibrosis-Related Parameters (q-FP) to Model Disease Progression in Steato-Hepatitis,” *Hepatology* 65 (2017): 1891–1903.

16. F. Liu, J. M. Zhao, H. Y. Rao, et al., “Second Harmonic Generation Reveals Subtle Fibrosis Differences in Adult and Pediatric Nonalcoholic Fatty Liver Disease,” *American Journal of Clinical Pathology* 148 (2017): 502–512.

17. P. E. Chang, G. B. B. Goh, W. Q. Leow, L. Shen, K. H. Lim, and C. K. Tan, “Second Harmonic Generation Microscopy Provides Accurate Auto-Mated Staging of Liver Fibrosis in Patients With Non-Alcoholic Fatty Liver Disease,” *PLoS One* 13 (2018): e0199166.

18. N. Ng, D. Tai, Y. Ren, et al., “Second-Harmonic Generated Quantifiable Fibrosis Parameters Provide Signatures for Disease Progression and Regression in Nonalcoholic Fatty Liver Disease,” *Clinical Pathology* 16 (2023): 1–12.

19. N. Otsu, “A Threshold Selection Method From Gray-Level Histograms,” *IEEE Transactions on Systems, Man, and Cybernetics* 9 (1979): 62–66.

20. P. Soille, *Morphological Image Analysis-Principles and Applications* (Springer-Verlag New York, Inc., 2003).

21. R. J. Lewis, “An Introduction to Classification and Regression Tree. (CART) Analysis. Annual Meeting of the Society for Academic Emergency Medicine,” 2000.

22. L. Lam, S. W. Lee, and C. Y. Suen, “Thinning Methodologies-A Comprehensive Survey,” *IEEE Transactions on Pattern Analysis and Machine Intelligence* 14, no. 9 (1992): 869–885.

23. T. Rückstieß, C. Osendorfer, and P. van der Smagt, “Sequential Feature Selection for Classification,” in *AI 2011: Advances in Artificial Intelligence*, vol. 7106, ed. D. Wang and M. Reynolds (Springer, 2011), 132–141.

24. F. Liu, G. B. Goh, D. Tiniakos, et al., “qFIBS: An Automated Technique for Quantitative Evaluation of Fibrosis, Inflammation, Ballooning, and Steatosis in Patients With Nonalcoholic Steatohepatitis,” *Hepatology* 71, no. 6 (2020): 1953–1966.